EFDA–JET–CP(11)04/02

M. Groth, G.D. Porter, T.D. Rognlien, S. Wiesen, M. Wischmeier, M.N.A. Beurskens, X. Bonnin, B.D. Bray, S. Brezinsek, N.H. Brooks, D.P. Coster, T. Eich, M.E. Fenstermacher, C. Fuchs, R.A. Groebner, D. Harting, A. Huber, S. Jachmich, A. Kallenbach, C.J. Lasnier, A.W. Leonard, A. Meigs, H.W. Müller, M.E. Rensink, D.L. Rudakov, J.G. Watkins, E. Wolfrum, the DIII-D and ASDEX Upgrade Teams and JET EFDA contributors

Poloidal Distribution of Recycling Sources and Core Plasma Fueling in DIII-D, ASDEX-Upgrade, and JET L-mode Plasmas

Poloidal Distribution of Recycling Sources and Core Plasma Fueling in DIII-D, ASDEX-Upgrade, and JET L-mode Plasmas

M. Groth[1,2], G.D. Porter[2], T.D. Rognlien[2], S. Wiesen[3], M. Wischmeier[4], M.N.A. Beurskens[5], X. Bonnin[6], B.D. Bray[7], S. Brezinsek[3], N.H. Brooks[7], D.P. Coster[4], T. Eich[4], M.E. Fenstermacher[2], C. Fuchs[4], R.A. Groebner[7], D. Harting[3], A. Huber[3], S. Jachmich[8], A. Kallenbach[4], C.J. Lasnier[2], A.W. Leonard[7], A. Meigs[5], H.W. Müller[4], M.E. Rensink[2], D.L. Rudakov[9], J.G. Watkins[10], E. Wolfrum[4], the DIII-D and ASDEX Upgrade Teams and JET EFDA contributors*

JET-EFDA, Culham Science Centre, OX14 3DB, Abingdon, UK

[1]*Aalto University, Association EURATOM-Tekes, Otakaari 4, 02015 Espoo, Finland*
[2]*Lawrence Livermore National Laboratory, CA, USA*
[3]*EURATOM-CCFE Fusion Association, Culham Science Centre, OX14 3DB, Abingdon, OXON, UK*
[4]*Forschungszentrum Jülich GmbH, EURATOM-Assoziation, TEC, Jülich, Germany*
[5]*EURATOM/CCFE - Fusion Association, Culham Science Centre, Abingdon, UK.*
[6]*LSPM CNRS, Université Paris 13, France.*
[7]*General Atomics, San Diego, CA, USA.*
[8]*Association 'Euratom-Belgian state', Ecole Royale Militaire, Brussels, Belgium.*
[9]*University of California San Diego, La Jolla, USA.*
[10]*Sandia National Laboratories, Albuquerque, NM, USA.*
** See annex of F. Romanelli et al, "Overview of JET Results", (23rd IAEA Fusion Energy Conference, Daejon, Republic of Korea (2010)).*

Preprint of Paper to be submitted for publication in Proceedings of the
38th EPS Conference on Plasma Physics
Strasbourg, France
(27th June 2011 - 1st July 2011)

ABSTRACT

Deuterium fueling profiles across the separatrix have been calculated with the edge fluid codes UEDGE, SOLPS, and EDGE2D/EIRENE for lower single null, ohmic and low-confinement plasmas in DIII-D, ASDEX Upgrade, and JET. The fueling profiles generally peak near the divertor x-point, and broader profiles are predicted for the open divertor geometry and horizontal targets in DIII-D than for the more closed geometries and vertical targets in AUG and JET. Significant fueling from the low field side midplane may also occur when assuming strong radial ion transport in the far scrape-off layer. The dependence of the fueling profiles on upstream density is investigated for all three devices, and between the different codes for a single device. The validity of the predictions is assessed for the DIII-D configuration by comparing the measured ion current to the main chamber walls at the low field side and divertor targets, and deuterium emission profiles across the divertor legs, and the high field and low field side midplane regions to those calculated by UEDGE and SOLPS.

1. INTRODUCTION

The poloidal profile of hydrogen (or isotopes thereof) fueling across the separatrix is predicted to impact the pedestal in high-confinement mode (H-mode) plasmas [1],[2] and thus the plasma performance in present and future fusion devices. Based on a fueling model derived by Mahdavi et al. [1] for both low-confinement mode (L-mode) and H-mode plasmas, the width and height of the density pedestal are determined by the penetration depth of neutrals from the Scrape-Off Layer (SOL) into the core plasma and radial outward diffusion of ions across the pedestal. A poloidal weighting parameter was introduced to account for poloidal magnetic flux expansion in the vicinity of the divertor x-point; typically, for diverted discharges in present tokamaks poloidal flux expansion is factors of 5 to 10 higher at the x-point region than at the Low (toroidal) Field Side (LFS) midplane. According to this model, fueling from regions of low flux expansion is advantageous in achieving high pedestal densities.

Independent of the confinement regime, the primary locations of neutrals crossing the separatrix are determined by where neutrals originate and how they attenuate within the SOL. In diverted configurations, most of the ion flux is intentionally directed toward the divertor plates, hence dominant recycling at the plates will lead to a strong neutral source in the divertor. Previous studies in DIII-D [3] showed that deuterium release, as both molecules and atoms, is two to three orders of magnitude higher from the divertor region than from the main chamber walls. The resulting poloidal peaking of the neutral flux at the x-point subsequently depends on the attenuation of neutrals within the divertor plasma, on the leakage of neutrals through the SOL due to multiple charge-exchange processes, and on the leakage in the halo plasma region between the SOL and the vessel walls. In detached divertor conditions, the plasma temperature in front of the divertor plates is as low as 1eV, and thus the neutral source expands from the plates to regions close to the x-point. Concomitantly, the ionization mean free path is long, and may exceed the dimensions of the divertor structure. Direct assessment of the neutral density along the upstream separatrix, however, is hampered by the lack of measurements. To further elucidate poloidal asymmetries in neutral density, measurements

at multiple poloidal locations are required.

The complexity of determining the neutral fueling profile may be addressed by numerical studies using two-dimensional (2-D) fluid codes, such as UEDGE [4], SOLPS [5], and EDGE2D [6], covering both the SOL and the pedestal regions. These codes utilize measured plasma conditions in the main chamber (typically taken at the LFS midplane) and calculate the plasma conditions elsewhere, including the ion fluxes to main chamber and divertor surfaces, and deuterium emission. The resulting neutral fluxes are then followed with either a fluid (UEDGE) or kinetic model (EIRENE [7] within SOLPS and EDGE2D), iteratively coupled to the plasma code. The approach critically hinges on the success of simultaneously replicating the measurements. In turn, sufficiently diagnosed plasmas are required to validate the numerical solutions, and to determine the sensitivity of applied models and boundary conditions on the resulting neutral fluxes. Simulations of the neutral fueling in L-mode and H-mode plasmas in DIII-D with the DEGAS [8] and EIRENE codes previously indicated strong fueling from the high (toroidal) field side (HFS) divertor x-point region, [9],[10],[11],[12]. Strong fueling from the HFS divertor x-point region was also calculated interpretatively for ASDEX Upgrade (AUG) using the 1-D neutral model KN1D [13].

To expand this work and further investigate the effect of divertor detachment, and divertor geometry and size, a set of ohmic and L-mode plasmas in DIII-D, AUG, and JET were chosen, on the grounds of being quiescent (i.e., no SOL perturbations due to edge localized modes (ELMs)) and being sufficiently diagnosed. Simulating L-mode plasmas may not directly address the issue of H-mode density pedestal formation, but allow the predictions to be tested against the fueling model proposed in [1], which is independent of the core confinement mode. The experimental setup and results were previously described in [14]. Common to all three devices was the magnetic configuration (lower single null with the ion gradient drift ($\mathbf{B}\times\nabla B$) direction toward the bottom), and a scan of upstream density to obtain attached, high-recycling, and detached (DIII-D and AUG only) divertor conditions. At the time of the experiments compared here, all three devices were operating with carbon-based plasma-facing components in the divertor; AUG was operating with tungsten main chamber walls, while in DIII-D and JET the plasma-facing components were carbon. On the other hand, the three tokamaks differ in physical dimensions: DIII-D and AUG are medium-size devices of similar size, while their divertor geometries were open with a horizontal divertor plasma configuration (DIII-D) and closed with a vertical configuration (AUG). JET is a large-size tokamak, and its characteristic divertor width and height are about 50% longer than those of DIII-D and AUG. A vertical divertor target configuration was investigated, similar to the one in AUG. The coil setup of each device, and the choice of plasma current and toroidal magnetic field resulted in different poloidal flux expansion around the x-point: the DIII-D case has the widest average flux expansion of approximately 7.0, versus JET of 5.2 and AUG of 3.6.

2. UEDGE PREDICTIONS OF CORE PLASMA FUELING PROFILES FOR DIII-D, AUG, AND JET

The density scans in DIII-D, AUG, and JET were simulated with the 2-D multi-fluid edge code

UEDGE [4], including **E×B** and **B×∇B** cross-field drifts [15]. The transport of deuterium atoms is described by fluid and momentum continuity equations [16]; molecules are not included. As similar as possible assumptions on plasma transport and boundary conditions were made in simulating all three devices, and systematically varied to account for differences in the machine setup (e.g., main chamber materials and pumping conditions) and measured upstream conditions (e.g., input power, density and temperature profiles). Details on the simulation setups may be found in [14]. It is important to emphasize that radial diffusion coefficients in excess of $5 m^2/s$ were assumed in the far SOL for DIII-D, while lower coefficients ($< 2 m^2/s$) of were chosen for AUG and JET. This choice was entirely driven by the availability of detailed measurements of the electron density with a reciprocating probe and D_α emission in the far SOL in DIII-D; Thomson scattering profile measurements were available for all three devices. The effect of classical cross-field drifts was investigated by running cases without and with these terms activated. Carbon sputtering and transport were included in the simulations, utilizes chemical sputtering yields published by Haasz and Davis [17].

The predicted atomic deuterium flux profiles across the separatrix ($\Gamma_{D0,sep}$) are peaked in the region poloidally upstream of the HFS x-point and at the LFS midplane (Fig.1). At the lowest density, the profiles also peak poloidally upstream of the LFS x-point. With increasing upstream density, $\Gamma_{D0,sep}$ increases both at the HFS x-point and LFS midplane, and decreases at the LFS x-point. Including cross-field drifts approximately doubles $\Gamma_{D0,sep}$ in the HFS region, while a 30% reduction in $\Gamma_{D0,sep}$ is observed at the LFS midplane region for the two highest density cases. The increase in $\Gamma_{D0,sep}$ at the LFS midplane region is a direct consequence of the radial diffusion model chosen for the far SOL region. By lowering $D_{\perp,farSOL}$ from 10 m^2/s to 2 m^2/s, the peak $\Gamma_{D0,sep}$ may be reduced to 5×10^{19} $m^{-2}s^{-1}$, however, at the expense of moving the predicted wall currents and D_α emission at the LFS midplane away from their corresponding measurements. The increase in $\Gamma_{D0,sep}$ at HFS x-point when drifts are included is due lower temperatures in the HFS divertor plasma for the same upstream separatrix density. Both results will be re-examined in section 3.

With UEDGE, neutral fueling is predicted to be strongly peaked at the HFS x-point for AUG and JET, while significantly broader fueling profiles are calculated for DIII-D (Fig.2). The peak in $\Gamma_{D0,sep}$ at the HFS is observed further upstream for DIII-D than for AUG and JET, indicative of stronger neutral attenuation near the x-point, possibly due to larger flux expansion for the DIII-D configuration. With increasing upstream density, $\Gamma_{D0,sep}$ increases near the HFS x-point, and decreases near the LFS x-point. As noted for the DIII-D cases, the choice of $D_{\perp,farSOL}$ sets $\Gamma_{D0,sep}$ at the LFS midplane: $\Gamma_{D0,sep}$ is highest for DIII-D, however, assuming a similar (and lower) $D_{\perp,farSOL}$ (of about 2 m^2/s) for the three devices, $\Gamma_{D0,sep}$ at the LFS midplane can be made essentially the same.

3. SOLPS PREDICTIONS OF CORE PLASMA FUELING FOR DIII-D AND AUG

To investigate the effect of fluid versus kinetic treatment of the neutrals, the fluid code SOLPS [5] was used to simulate the density scans in DIII-D and AUG. The primary intent of this comparison was to determine qualitative and order-of-magnitude differences in the predictions of $\Gamma_{D0,sep}$ when using otherwise similar-as-possible assumptions in the codes. The plasma solver in SOLPS

(B2.5) is iteratively coupled to the neutral Monte-Carlo code EIRENE (here, version of 1999), including deuterium atoms and molecules. A purely diffusive radial transport model was adapted, with transport coefficients similar to those chosen for UEDGE, to reproduce the measured profiles of electron density and temperature, and ion temperature at the LFS midplane. At the time of this report, SOLPS solutions without the cross-field drifts only were obtained for DIII-D, while for the AUG cases simulations without and with the drifts already existed [18]. Carbon was included in the simulations, and a constant chemical sputtering yield of 1% was assumed in this study.

The poloidal fueling profiles predicted by SOLPS for DIII-D are significantly more localized near both the HFS and LFS x-points than those calculated by UEDGE (Fig.3a versus Fig.1a). With increasing density, the peak $\Gamma_{D0,sep}$ at both the HFS and LFS x-points increase, and the region of strong fueling extends poloidally further upstream, both along the HFS and LFS separatrices. As in the UEDGE simulations, the peak $\Gamma_{D0,sep}$ is predicted poloidally upstream of the x-points, and not directly adjacent to it.

The poloidal fueling profiles predicted by SOLPS for AUG are significantly more localized at the divertor x-point than those for DIII-D, and the peak $\Gamma_{D0,sep}$ is observed directly adjacent to the x-point for all three densities considered (Fig.3b). With increasing density the fueling profile broadens at the HFS, while it remains narrow at the LFS. As observed in the DIII-D simulations, the peak $\Gamma_{D0,sep}$ at the LFS is predicted higher with SOLPS than with UEDGE. It is important to note that SOLPS simulations without and with drifts produce very similar ion fluxes to the divertor plates and divertor plasma condition [18], resulting in almost identical neutral fueling profiles. For nearly identical L-mode plasmas in AUG strong fueling from the HFS SOL was also inferred by Harhausen et al. [13], utilizing 2-D D_α emission measurements and simulations with the 1-D kinetic neutral code KN1D [19]. The absolute deuterium fluxes from K1ND exceed the SOLPS predictions by factors 2 to 3, and those of UEDGE by an order of magnitude.

4. COMPARISON OF PREDICTED ION FLUXES AND D_α EMISSION FROM UEDGE AND SOLPS TO DIII-D DATA

To assess the validity of the UEDGE and SOLPS predictions for $\Gamma_{D0,sep}$, the code results were compared to the measured ion currents to the HFS and LFS targets, the estimated currents across the LFS SOL, and D_α measurements across the divertor legs. Due to required brevity of this publication, emphasis is given to the measurements in DIII-D, which provided additional D_α measurements along the HFS SOL between the x-point and the midplane, and radially across the LFS midplane. Both UEDGE and SOLPS overestimate the ion currents (I_{div}) to the HFS and LFS for high-recycling and detached divertor regimes (Fig. 4). The predicted I_{div} monotonically increase with upstream density, and only saturate and decrease at the highest density; I_{div} predicted by SOLPS are approximately 30 - 50% higher than by UEDGE. The inclusion of cross-field drifts in UEDGE results in saturation of I_{div} at the HFS at 30% lower upstream density and a stronger reduction in I_{div} at the highest upstream density (Fig.4a). To reproduce the estimated ion current across the flux surface defined by the upper outer limiter and the lower divertor baffle ('window frame current'

[20]), increased radial transport (as imposed by raising $D_{\perp,farSOL}$) is required (Fig.4c). Assuming a $D_{\perp,farSOL}$ of 8 m^2/s reproduces the inferred currents while a $D_{\perp,farSOL}$ of $2m^2/s$ falls short of the experimental value by a factor of 4. Values of $D_{\perp,farSOL}$ in excess of $8m^2/s$ would be required in SOLPS to match the experimentally inferred ion currents.

Inclusion of the drifts in UEDGE raises the D_α emission in the HFS divertor and moves the solution to within 20% of the measured emission; however, the predicted D_α emission at the LFS remains a factor of 4 lower than what is observed experimentally (Fig. 5a for a high-density case). Due to higher ion currents to the LFS target predicted, and the inclusion of molecules and their dissociation chain [21], SOLPS produces a factor of 2 higher D_α emission across the LFS divertor. Given the discrepancy of I_{div} to the LFS targets between the experiments and simulations, the agreement in D_α emission may even be surprising: D_α emission is produced by both ionization and recombination processes, and thus a convolved function of neutral, electron, and ion density as well as electron temperature, all taken along the lines-of-sight. Both codes predict ionization-dominated LFS divertor plasmas, with the peak in deuterium ionization remaining close to the LFS plate, while measurements with the divertor Thomson scattering system show a strongly recombining plasma in front of the plate.

Stronger detachment of the HFS divertor plasma predicted by UEDGE with the drifts included results in higher D_α emission upstream of the HFS divertor x-point reproducing the measurements (Fig.5b). Both UEDGE and SOLPS without drifts fall short on reproducing the measured D_α emission by factors 2 to 3. One would anticipate that inclusion of the drifts in SOLPS would produce a similar effect as observed in UEDGE, and thus yield stronger detachment at the HFS and better agreement with the data.

The predicted D_α emission at the LFS midplane by SOLPS reproduces the measured emission profile both qualitative and quantitatively, while UEDGE calculates lower emission close to the separatrix, and higher emission in the far SOL (Fig.5c). However, the agreement between the data and UEDGE predictions are within 50%. Coster et al. [22] showed previously, for B2.5 coupled to its fluid neutral model, that modification of the neutral limits and of the decay length of the ion temperature raises the neutral density near the separatrix, which in turn would raise the D_α emission. Such modification has not yet been attempted for UEDGE. More importantly, to reproduce the D_α emission in the far SOL reduction of $D_{\perp,farSOL}$ from 8 m^2/s to 2 m^2/s reduces the D_α emission in the far SOL by 50% for SOLPS, and by a factor of 4 across the entire profile for UEDGE.

5. EDGE2D/EIRENE PREDICTIONS OF CORE PLASMA FUELING FOR JET

To assess neutral fueling with a coupled fluid plasma-kinetic neutral code for the JET configuration, the EDGE2D/EIRENE [6], [23] code was used. The setup of the radial transport model followed the same philosophy as for UEDGE and SOLPS: a diffusive model was chosen with the transport coefficients having a minimum across the separatrix to form a transport barrier there. The transport coefficients were modified until the calculated profiles for electron density and temperature at the LFS midplane match the profiles measured by high-resolution Thomson scattering. Since the radial

extent of the measurements is limited to the near-separatrix SOL, diffusion coefficients of 1 m^2/s and 10 m^2/s were assumed in the far SOL. Cross-field drifts are not included in the simulations. Carbon release due to physical and chemical sputtering, assuming the Roth 2004 chemical sputtering yields [24], and carbon transport are included in this study.

With increasing upstream density the EDGE2D/EIRENE predicted fueling profiles become poloidally more uniform (Fig.6). At low upstream density the fueling profile is strongly peaked at both the HFS and LFS x-point regions. As the upstream density increases, the profile broadens at the HFS SOL upstream of the x-point, both total fueling and the peak $\Gamma_{D0,sep}$ increase at LFS midplane, and $\Gamma_{D0,sep}$ decreases at the LFS x-point region. These predictions are qualitatively consistent with those from UEDGE without the drifts (not shown in this publication).

DISCUSSION

Simulations of DIII-D, AUG, and JET L-mode plasmas with UEDGE, SOLPS, and EDGE2D/EIRENE commonly indicate that the regions adjacent to both the HFS and LFS divertor x-point are the regions of strongest neutral flux across the separatrix. The fueling is therefore determined by ion recycling at the divertor target plates and recombination within the divertor plasma, and subsequent charge-exchange transport of neutrals from the divertor into SOL upstream of the x-point. These results are qualitatively and quantitatively consistent with previous predictions for DIII-D [9], [10], [11]. For low upstream densities and attached divertor conditions, strongly peaked fueling profiles are predicted by all three codes for all three devices. As the upstream density is increased, and the plasma temperatures in front of the plates fall below 1 eV, the predictions deviate significantly from code to code.

Elucidating the issue of divertor recycling and divertor x-point fueling ultimately returns to the question of how accurately the ion fluxes to the targets and the 2-D divertor conditions are reproduced by the codes. As shown in Fig. 4 for DIII-D, both UEDGE and SOLPS overestimate the ion fluxes to the targets. The same conclusion was already drawn by Wischmeier et al. for SOLPS simulating the same discharge series in DIII-D and AUG [18] and, more recently, an almost identical, yet better diagnosed L-mode density scan in AUG [26]. Further reduction of the predicted ion currents to the targets at high upstream density for all three devices with UEDGE, by increasing the chemical sputtering yields at the plates above the Haasz-Davis yields, resulted in overestimating the measured emission of low charge state carbon in the divertor [14]. Saturation of the ion currents to the target plates was also observed only at the highest achievable density with EDGE2D/EIRENE for the JET configuration, and transiently the currents can be reduced when applying collisionality-dependent transport coefficients in the perpendicular-**B** direction [29]. Not being able to adequately reproduce the dependence of the ion currents to the targets with upstream density appears to be a fundamental issue with fluid codes, and based on these and previous studies may not necessarily be attributed to the choice of the neutral model only. The presence of super-thermal electrons in the divertor plasma, resulting in an increase in the recombination rates, was identified by Coster et al. [30] as a possible mechanism to elucidate the discrepancy between the measured and predicted ion currents to the wall.

Further comparison of measured 2-D profiles of emission from low charge state carbon in the HFS and LFS divertors in DIII-D show that for given (experimental) upstream conditions, UEDGE predicts higher temperatures in both divertor legs than those inferred from the emission zones. Inclusion of cross-field drifts in the UEDGE simulations reduces the temperature in front of the HFS divertor [15], [25] and moves the ionization front off to the HFS target. However, the location of the ionization front still remains closer to the plate than inferred from the measured carbon emission profile. Cold and strongly recombining HFS divertor plasmas with the ionization front at the HFS x-point are obtained at upstream densities 20–50 % higher than those measured. For the LFS divertor leg, both UEDGE and SOLPS predict the peak in n_e to occur close to the LFS plate, while 2-D measurements with the DIII-D divertor Thomson scattering system put the peak close to the LFS divertor x-point. In the UEDGE simulations, the ionization front moves almost instantaneously from the LFS plate to the x-point as the density limit is approached, which typically terminates the simulation. With SOLPS, a more continuous transition of the ionization front from the LFS plate to the x-point is observed. Consequently, stronger fueling from the LFS x-point region is predicted by SOLPS than by UEDGE (Figures 1 and 3).

All three codes indicate that ion recycling at the LFS main chamber wall may result in significant fueling at the LFS midplane (Figs.1, 3b, and 6). For both UEDGE and SOLPS to match the ion current across the outer SOL in the main chamber in DIII-D (inferred from a 'window frame' analysis [20]), diffusion coefficients in excess of 5 m^2/s had to be imposed in the far SOL. Clearly, a physics-based radial transport model is needed to adequately predict main chamber recycling. By applying a non-diffusive transport model with radially increasing convective velocities, Pigarov et al. [27], [28] previously showed that the core plasma is predominantly fueled by neutrals originating at the LFS midplane wall. A similar effect is observed by introducing collisionality-dependent diffusivities into EDGE2D/EIRENE [29]. Elucidating the issue of core fueling due to main chamber recycling will eventually require a turbulent description of radial transport, with grids extended to the walls, and validated against ion flux measurements at multiple poloidal locations.

CONCLUSIONS

Simulations of lower single null, ohmic and L-mode plasmas in DIII-D, AUG, and JET with the UEDGE, SOLPS, and EDGE2D/EIRENE codes predict that the flux of neutrals crossing the separatrix is localized at or close to the divertor x-point. Following equation 8 of ref. [2], these results would unfavorably scale toward high pedestal densities. Depending on the strength of radial transport in the far SOL, the calculated fueling profiles also peak at the LFS midplane. The open divertor geometry with horizontal targets in DIII-D is predicted by UEDGE and SOLPS to produce broader fueling profiles than the closed geometries with vertical targets in AUG and JET, as neutrals are preferentially released toward the main chamber. In configurations with wider flux expansion, the peak in the fueling profile occurs poloidally upstream of the divertor x-point, and not directly adjacent to it, consistent with assumption of stronger neutral attenuation at the x-point as the flux expansion is increased. With increasing upstream density, fueling from the HFS divertor x-point

region is predicted to increase (UEDGE for all three devices, SOLPS for DIII-D and AUG) or to remain constant (EDGE2D/EIRENE for JET). The fueling profiles along the HFS SOL are generally broader at high upstream densities than at low upstream density. Fueling from the LFS divertor x-point region was found to decrease (UEDGE for all three devices, EDGE2D/EIRENE for JET), remain constant (SOLPS for AUG), or increase (SOLPS for DIII-D). Broadening of the fueling profile at the LFS x-point with increasing upstream density is observed with SOLPS for DIII-D, while the narrow fueling profiles right at the LFS x-point are predicted by EDGE2D/EIRENE for JET. The predicted fueling profiles are a direct consequence of the calculated ion recycling at the target plates, volume recombination within the divertor legs, and the plasma conditions in the divertor legs, in general. Divertor solutions with temperatures at 1eV at the plate were obtained with all three codes for all three devices. However, the predicted ion currents to the plates generally do not agree with the reduced currents observed experimentally at high upstream density. For high upstream densities in DIII-D, comparison of measured electron density in the LFS divertor against UEDGE and SOLPS simulations indicate that the ionization front remains close to the plate, whereas experimentally it is observed just downstream of the x-point. These fundamental issues remain outstanding and require inclusion of other physics process, such as super-thermal electrons. Inclusion of cross-field drifts results in closer approximation of measured divertor asymmetries (UEDGE for DIII-D and AUG), but in other cases it did not significantly change the divertor solutions (SOLPS for AUG). Assuming stronger radial transport in the far SOL, motivated either by matching experimental data or testing a physics model, results in an increase in fueling from the LFS midplane region. Direct measurements of ion fluxes to main chamber surfaces and simulations on grids extending to the main chamber are required to corroborate these predictions.

ACKNOWLEDGMENTS

This work was supported by EURATOM and carried out within the framework of the European Fusion Development Agreement. The views and opinions expressed herein do not necessarily reflect those of the European Commission. This work was also performed in part under the auspices of the U.S. Department of Energy by Lawrence Livermore National Laboratory under Contract DE-AC52-07NA27344, DE-FG02-07ER54917, DE-AC05-00OR22725 and DE-AC04-94AL85000.

References

[1]. M.A. Mahdavi et al., Physics of Plasmas **10** (2003) 3984.
[2]. R.J. Groebner et al., Nuclear Fusion **44** (2004) 204.
[3]. E.M. Hollmann et al., Physics of Plasmas **48** (2006) 1165.
[4]. T.D. Rognlien et al., Journal of Nuclear Materials **196-198** (1992) 347.
[5]. R. Schneider et al., Contributions to Plasma Physics **46** (2006) 3.
[6]. A. Taroni et al., Contributions to Plasma Physics **32** (1992) 438.
[7]. D. Reiter et al., Journal of Nuclear Materials **196-198** (1992) 241; http://www.eirene.de.
[8]. D.B. Heifetz et al., Journal of Computational Physics **46** (1982) 309.

[9]. L.W. Owen et al., Journal of Nuclear Materials **337-339** (2005) 410.
[10]. M. Groth et al., Journal of Nuclear Materials **337-339** (2005) 425.
[11]. A.W. Leonard et al., Journal of Nuclear Materials **390-391** (2009) 470.
[12]. J.D. Elder et al., Bulletin of the American Physical Society **54** (2009) TP8.00030.
[13]. J. Harhausen et al., Plasma Physics and Controlled Fusion **53** (2011) 025002.
[14]. M. Groth et al., Journal of Nuclear Materials (2010), doi. 10.1016/j.jnucmat.2010.10.024
[15]. T.D. Rognlien et al., Physics of Plasmas **6** (1999) 1851.
[16]. T.D. Rognlien et al., Contributions to Plasma Physics **36** (1996) 105.
[17]. J.W. Davis et al., Journal of Nuclear Materials **241-243** (1997) 37.
[18]. M. Wischmeier et al., Journal of Nuclear Materials **390-391** (2009) 250.
[19]. B. LaBombard B *Plasma Science and Fusion Center Research Report* PSFC-RR-01-3, year 2001
[20]. D.G. Whyte et al., Plasma Physics and Controlled Fusion **47** (2005) 1579.
[21]. S. Brezinsek et al., Plasma Physics and Controlled Fusion **47** (2005) 1.
[22]. D.P. Coster et al., Physica Scripta **T108** (2004) 7.
[23]. S. Wiesen, EDGE2D/EIRENE code interface report, JET ITC report 2006, http://www.eirene.de/e2deir_report_30jun06.pdf.
[24]. J. Roth et al., Nuclear Fusion **44** (2004) L21.
[25]. A.V. Chankin et al., Plasma Physics and Controlled Fusion **38** (1996) 1579.
[26]. M. Wischmeier et al., Journal of Nuclear Materials (2010), doi. 10.1016/j.jnucmat.2011.02.020
[27]. A. Yu. Pigarov et al., Physics of Plasmas **9** (2002) 1287.
[28]. A. Yu. Pigarov et al., Journal of Nuclear Materials **337-339** (2005) 371.
[29]. S. Wiesen et al., Journal of Nuclear Materials (2010), doi. 10.1016/j.jnucmat.2010.12.010
[30]. S. Wiesen et al., Journal of Nuclear Materials (2010), doi. 10.1016/j.jnucmat.2010.12.223
[31]. D. Buchenauer et al., Review Scientific Instruments **61** (1990) 2873.
[32]. R.J. Colchin et al., Review Scientific Instruments **74** (2003) 2068.
[33]. M. Groth et al., Rewiew Scientific Instruments **80** (2009) 033505.

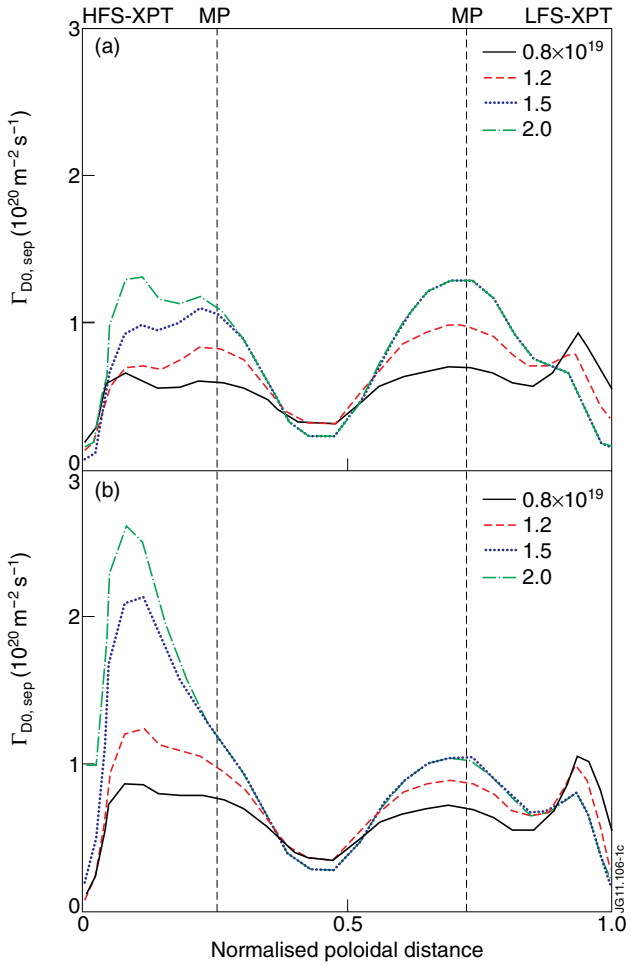

Figure 1: Poloidal profiles of the deuterium atomic flux across the separatrix as predicted by UEDGE for DIII-D. The abscissa runs along the separatrix from the HFS x-point to the LFS x-point, as indicated by the insert in (b). The colors correspond to the four electron densities at the separatrix. Results are shown for UEDGE without (a) and with cross-field drifts (b).

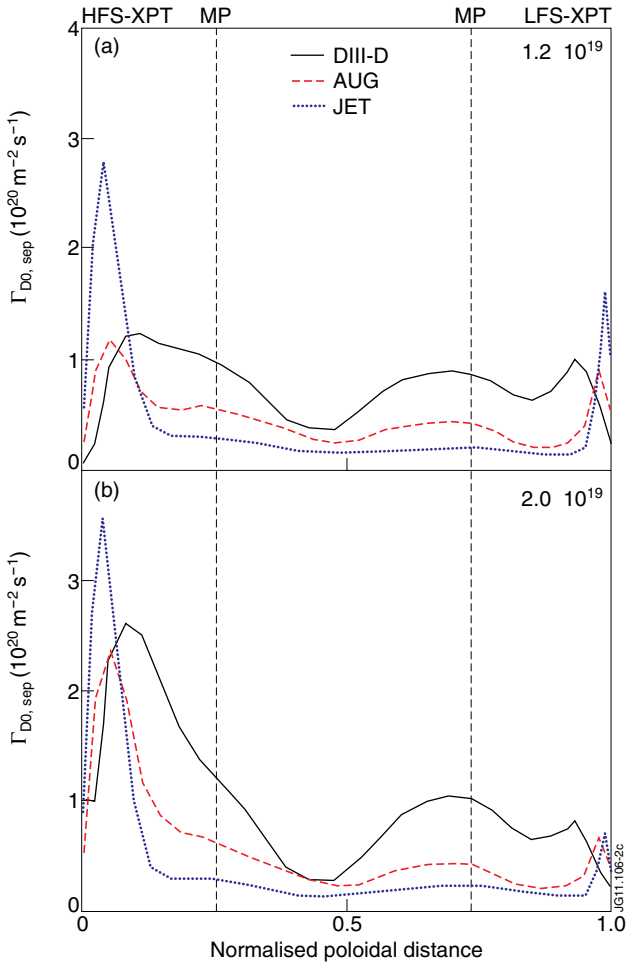

Figure 2: Predicted deuterium atomic flux across the separatrix from UEDGE for DIII-D (black), AUG (red), and JET (blue). Results obtained for two different densities are shown: (a) $n_{e,sep,LFS\text{-}mp} = 1.2\times10^{19}$ m^{-3} (high-recycling divertor conditions), and (b) $n_{e,sep,LFS\text{-}mp} = 2.0\times10^{19}$ m^{-3} (detached conditions).

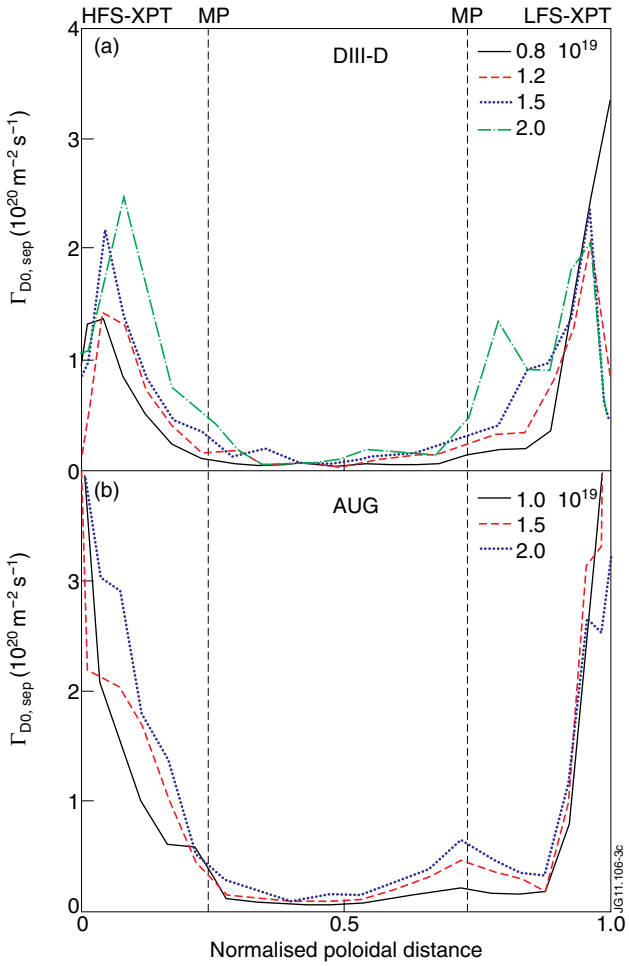

Figure 3: Predicted deuterium atomic flux across the separatrix from SOLPS: (a) without cross-field drifts for DIII-D, (b) with cross-field drifts for AUG.

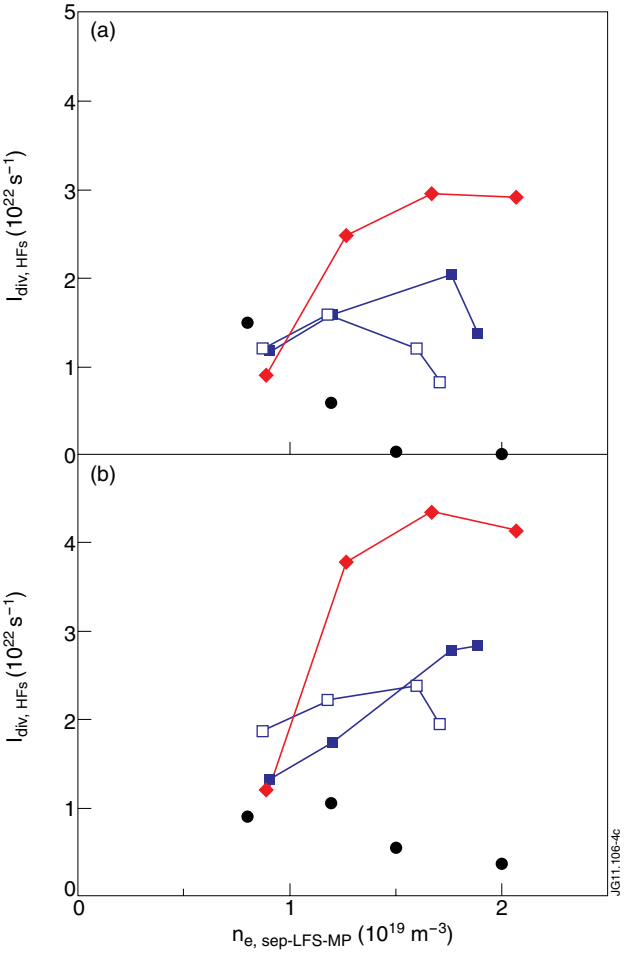

Figure 4: Measured and predicted ion currents to the HFS (a) and LFS (b) targets as a function upstream electron density at the separatrix of LFS midplane in DIII-D (#119919, 120350-58). The ion currents were measured with a Langmuir probe array embedded in the HFS and LFS target plates (black solid circles) [31]. The solid symbols refer to simulations without cross-field drifts, the open symbols to simulations including drifts. The blue symbols denote UEDGE simulations, red symbols SOLPS simulations. (c) Inferred and predicted ion currents across the outer SOL ('window frame' [20]) in DIII-D. The open red and green squares refer to UEDGE simulations with drifts and $D_{\perp,farSOL}$ = 8m^2/s and 2m^2/s, respectively. The closed blue and green diamonds refer to SOLPS simulations without drifts and $D_{\perp,farSOL}$ = 8m^2/s and 0.6m^2/s, respectively.

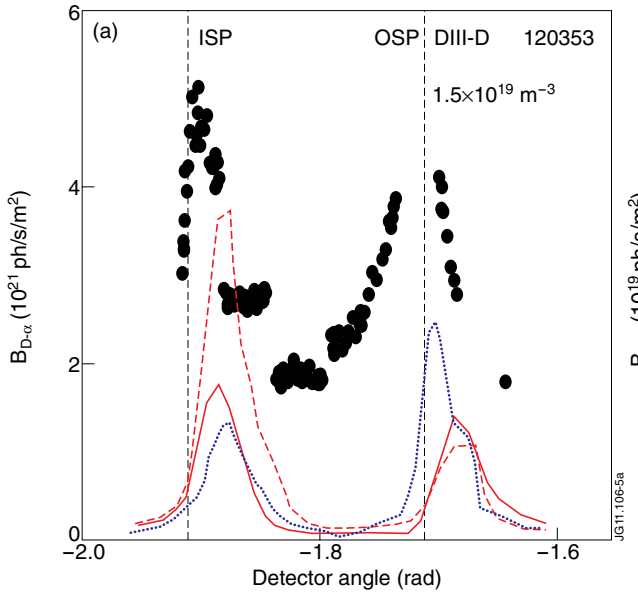

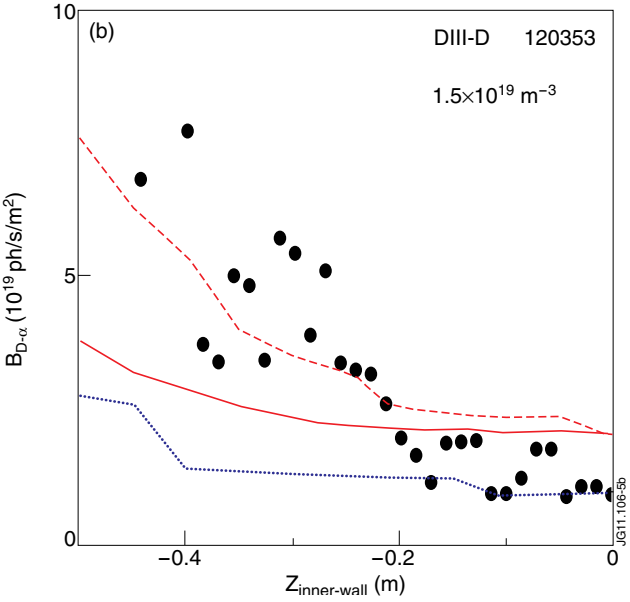

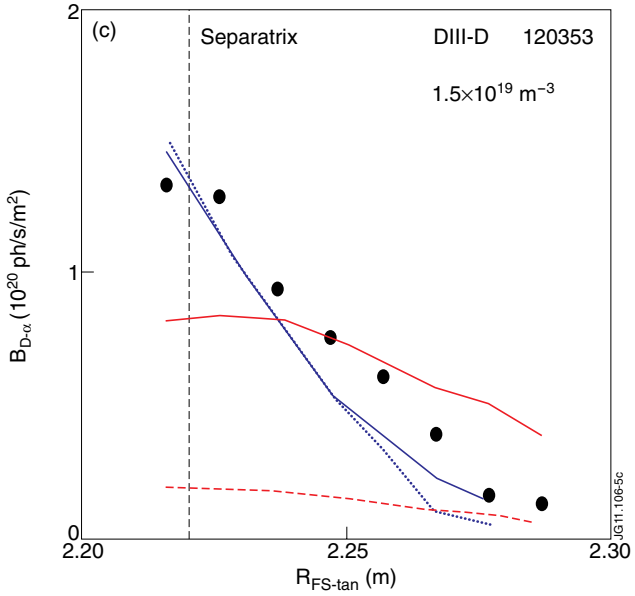

Figure 5: Measured and predicted D_α emission (brightness $B_{D\text{-}\alpha}$) in the lower divertor (a), HFS midplane (b), and LFS midplane (c) for a detached DIII-D case. The data were obtained with a vertically and a tangentially viewing photo-multiplier array (a, c [32]), and inferred from a tangentially viewing camera (b [33]). The data are plotted as functions of poloidal angle along the target plate wrt. the detector location (a), distance along the HFS wall wrt. midplane (b; x-point at Z= -1.1 m), and radius of point-of-tangency (c). In (a) and (b), predictions from UEDGE are shown in red, without (solid line) and with drifts (dashed), and SOLPS in blue. In (c), UEDGE (red) with $D_{\perp,farSOL}$ = $8m^2/s$ (solid) and $D_{\perp,farSOL}$ = $2m^2/s$ (dotted), and SOLPS (blue) simulations with $D_{\perp,farSOL}$ = $8m^2/s$ (solid) and $D_{\perp,farSOL}$ = $0.6m^2/s$ (dotted) are shown.

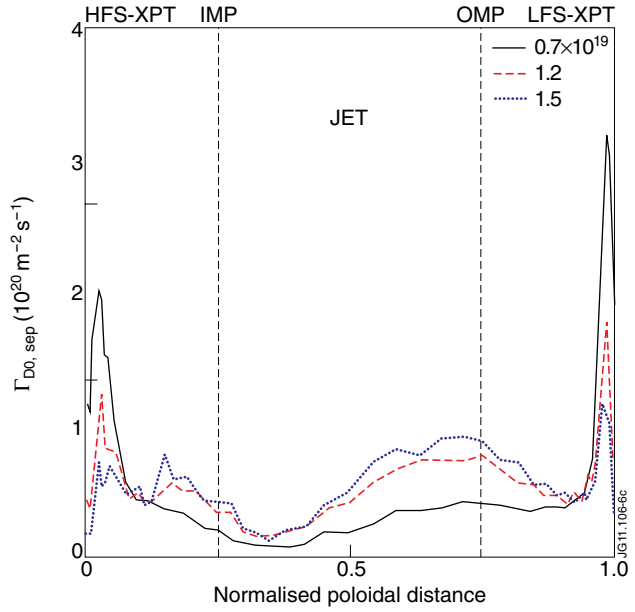

Figure 6: Predicted deuterium atomic flux across the separatrix from EDGE2D/EIRENE for the JET vertical target configuration.